



## Sources of Radioelement's and REEs in The Stream Sediments Bounded by Abu Rusheid Gneiss South Eastern Desert, Egypt

Saleh, W.H.

Received: 05/01/2019

Accepted: 19/02/2019

E.mail:drwafaahosny@live.com

### **ABSTRACT**

Abu Rusheid area forms a NW-SE antiformal structure and it is truncated by a major fault in the north-west along wadi sikeit. Granitic gneisses rocks are cross cut by NNW-SSW trending altered and mineralized shear zone. The study area is bounded by longitude  $34^{\circ} 48' 34^{\circ} 48' 30''$  E and latitude  $24^{\circ} 37' 24^{\circ} 38' N$ . This study aims to define sources and distribution of rare earth elements (REEs) and to describe the geochemical processes that govern mobility of U and valuable radioelements, which comes from leaching of more labile REEs bearing minerals of granitic gneisses rocks, cut by mineralized shear zone and green silicates mainly amphiboles (hornblende). And mineralization extension according to grain sizes in trace elements.

The REEs in the stream sediments illustrate more than one depth, samples on the surface have +ve Eu anomaly, while the middle samples on depth (0.5m, 1m) are similar to each other but differ from surface samples and chondrite, where they depleted in -ve Eu and Tm. The bottom depth, at (1.5m) europium, Tm began to increase. Negative europium anomaly maybe inherited from the felsic precursor rocks, a consequence of preferential leaching of Eu associated with the breakdown of feldspar (plagioclase) in direction of upstream sediments, suggesting that plagioclase free sediments are downstream in the studied area. At the surface contains high percentage of amphiboles, mainly (hornblende), iron oxide (goethite), few crystals of garnet, zircon and very fine monazite spots in

### **KEYWORDS**

*Abu Rushied,  
Lamprophyers,  
Granitic Gneiss,  
REEs, Radioelement's.*

allanite crystals embedded in silicate mineral. It is worthily that -ve Ce anomalies on surface and +ve Ce anomalies on (0.5m, 1m, 1.5m) depth, otherwise some light REEs elements are depleted and sometimes increase, this may be explained by combined effect of selective remobilization of Ce (IV) could have been initiated during cycles of the stream sediments where chemically reworked.

Under surficial weathering (epigene), the breakdown of allanite give monazite, clay minerals, cerianite and geothite where Ce and Nd rich allanite indicate concentrated LREEs during a late hydrothermal alteration, geothite on surface represents the secondary phase and is considered as the main criteria for chemical weathering. Whilst HREEs increase at (1m) depth where some minerals are concentrated (uranthorite, columbite), otherwise at depth (0.5m) and (1.5m) HREEs are similar due to the increase in zircon, xenotime, garnet and thorite. Enrichment in the middle REEs relative to the light and heavy REEs is chiefly controlled by hornblende, the REEs are compatible in hornblende in felsic and intermediate liquids and the highest partition coefficients are between Dy and Er. Mineralogical, this means the minerals seeming have undergone the dissolution of REEs in aqueous media at least once in history of REEs or might have been present in it, separated from the same original solution as liquid phase and solid phase.

The geochemical contour maps clarified the mineralization extension in deep levels from surface to (0.5m, 1m, 1.5m) of stream sediments according to distribution in Wadi Abu Rusheid. We notice that valuable trace elements take the same direction of peralkalic granitic gneisses and lamprophyre dikes where Zr, Y, Pb and Ga in size (-1 + 0.5) show the highest concentration in NNW-SSE direction and Nb in size (-0.5 + 0.25) take the same direction, while higher concentration of Zn in size (-0.25) take NE-NW, otherwise U take NW-SE and Th take NW to NS direction. Uranium show relatively increase in

(0.5m, 1m) depth respectively, while Th increase at (0.5m, 1m, 1.5m).

## INTRODUCTION

**A**bu Rusheid is located in the southern part of the Eastern Desert of Egypt, it lies to NE of the major shear zone known as the Nugrus thrust fault (**Grelling *et al.*, 1988**) or Nugrus strike-slip fault (**Fritz *et al.*, 2002**). **Grelling *et al.* (1993)** believe that shear zone in the pan African basement of the Eastern Desert may be related to compressional, as well as extensional stresses; however both types of deformation lead to antiformal structures on a regional scale. **Abd El Monem and Huraly (1979)** estimated the age date of psammitic gneisses by zircon detrital age which ranges between 1120 Ma and possibly 2060 Ma suggesting that this basement may be, the so called Nile Craton, while Abu Rusheid granites is  $610 \pm 20$  Ma determined by Rb - Sr method (**Moghaz *et al.*, 2004**).

The present study shows some mineralization and paragenesis. Also, geochemical studies of some valuable trace elements, in addition to measure U and Th with drawing contour maps indicating distribution, the direction of trace elements and U, Th on it. Finally explain sources and controlling factors of the REEs distribution.

### Geologic setting

Abu Rusheid area tectonostratigraphic succession forms a NW-SE antiformal structure, and it is truncated by a major fault in the north-west along wadi sikeit. The study area is bounded by longitude  $34^{\circ} 48' 34^{\circ} 48' 30''$  E and latitude  $24^{\circ} 37' 24^{\circ} 38'$  N (Fig. 1), occupied by igneous and metamorphic rocks, the succession from old to young are arranged as follows: (1) ophiolitic melange, consisting of ultramafic rocks and layered metagabbros with a meta-sedimentary matrix; (2) cataclastic rocks (peralkalic granitic gneisses) in the core of the granitic pluton,

which are composed of protomylonites, mylonites, ultramylonites and silicified ultramylonites, (3) mylonitic granites; and (4) post-granitic dikes and veins (Ibrahim *et al.*, 2004). The cataclastic rocks (per alkalic granitic gneisses) are cross cut by NNW-SSE trending altered and mineralized shear zone (Ali, 2012). The NNW-SSE lamprophyre dikes (L1 and L2, 0.5 – 1.0 m in width, 0.4-1.5 km in length) are located in the core of the cataclastic rocks (Ibrahim *et al.*, 2015). Then, wadi deposits (stream sediments and stream course).

### Materials and Methodology of Study

17 channel samples were collected from Wadi Abu Rusheid from pore holes having about 1m diameter, and 1.5m depth, on grid pattern of 25x100 m along profiles trending perpendicular to the wadi Fig.(2). The open pit divided vertically into 0.5, 1 and 1.5 meters. The average weight of each sample is about 10kg. The air-dried original sample was sieved using 2 mm screen. The obtained fraction less than 2mm was quartered using June's splitters of different chutes, down to about 250 gm. Then the obtained representative sample is washed carefully several times to clarify it from silt and clay. Hydrogen peroxide was used to get rid of the organic matters.

A representative sub-sample weighting about 60 gm was taken from each prepared sample by quartering for mineral separation. Separation was conducted using bromoform (Sp. Gr. 2.86g/cm<sup>3</sup>) and magnetic fractionation using a Frantz Isodynamic Magnetic Separator (Model L-1). Mineralogical identification of the mineral constituents recognized by stereomicroscope and their composition confirmed by environmental Semi-quantitative EDX chemical analysis, using Phillips XL-30 Environmental Scanning Electron Microscope (ESEM).

The 17 sample are split to 45 fraction samples (-0.25, -0.5 + 0.25, -1 + 0.5).The obtained fractions were analyzed for some trace elements. The elements were determined by X-ray fluorescence spec-

trimeter model (X-Uniqu II) by perssion 10%. The uranium and thorium were detected chemically by Control analysis method of uranium in the different aqueous stream solutions as well as in the product has been undertaken by the oxidimetric titration after its reduction using a standard solution of ammonium metavanadat (Mathew *et al.*, 2009). This has been possible after a prior uranium reduction step using ammonium ferrous sulfate. In this procedure, di-phenyl sulphonate has been used as indicator where upon its color would change to a slightly violet red color. Thorium is chemically determined by the colored method using Arsenazo-III, as an indicator. The colored method was performed using a spectrophotometer technique (Merczenko, 1986). REEs measured by inductively coupled plasma-mass spectrometry (ICP-MS) at the analytical laboratory (N.M.A).

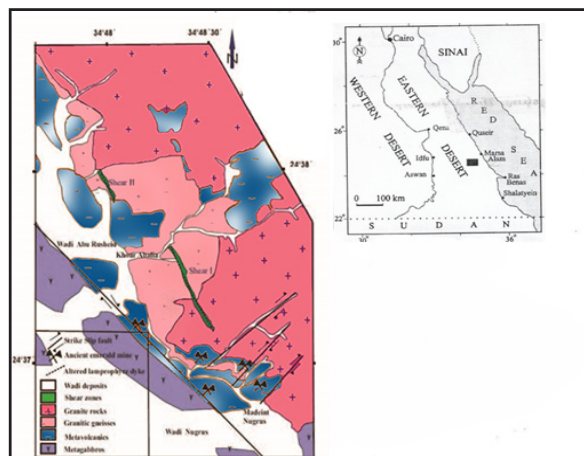


Fig. (1): Geological map of Abu Rusheid area (modified by Ali, 2012 after Ibrahim *et al.*, 2004).

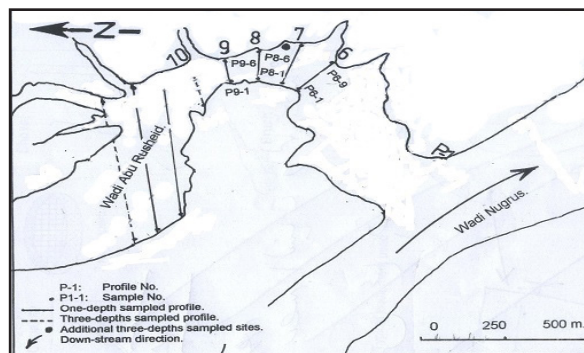


Fig. (2): Sample location map (Internal report N.M.A., 2003).

### *Mineralization and paragenesis*

Abu Rusheid area is subjected to hypothesis, was given by (Bugrov *et al.*, 1973). They concluded that radioactive rock is not a part of psammitic gneiss, but it is an apogranite (albitized granite) still concordant along the contact between the overlying schist and the under lying psammitic gneiss. This still represents an offshoot of a hidden apogranite intrusion.

Hilmy *et al.* (1990) suggested model for the re-distribution of minerals, proposed that mineralization might have taken place is believed to have involved the interaction between the gneiss formation enriched in elements, on one hand and the fluorine and hot gases phase. On the other hand, the breakdown of primary minerals such as zircon, columbite – tantalite etc. is attributed to a period of short duration of high interaction with the rock, rare elements Zr, Nb, Sn etc. The existence of U, Th and K in the original rock before alteration or mineralization can produce a hot rock district which will promote the convection process. The convection from a deep seated source was under considerable pressure. The gases infiltrated through fissures and cracks reaching the upper zone. Then the attraction process took place causing the redistribution of the mineralogical investigation of REE- minerals and radioactive – bearing minerals in the studied area.

Abdalla *et al.* (1996), ElAfandy *et al.* (2000) the granitic gneiss commonly display vertical petrographical zoning with a lower unaltered zone of alkali feldspar granites, a middle microclinized granite (zone of K-metasomatism). In addition, upper bleached grey to whitish albitized granite (zone of Na metasomatism). A small volume of graisenizy ( $H^+$  - metasomatized) of silicified granites.

Ali *et al.* (2011) studied the mineralogy and shear zone and proved on the basis of field evidence, textural relations and composition of ore minerals, that the main mineralization event was magmatic ( $629 \pm 5$  Ma, CHIME monazite), with later hydrothermal

alteration and local remobilization of high field - strength elements.

Ibrahim *et al.* (2015) studied the lamprophyre dikes and stated the NNW-SSE lamprophyre dikes ( $L_1$  and  $L_2$ ) are located in the core of the cataclastic rocks and the feldspars, micas in both  $L_1$  and  $L_2$  are partially altered to clay minerals (chemical traps) while the oxidation of sulfide minerals left ocelli (physical traps) usually filled by calcite and uranium minerals.

For the above reasons we studied the relation between some minerals on the surface and relatively some depths of stream sediments bounded by gneiss at 0.5, 1 and 1.5 meters. The collected samples composed of green silicate represented mainly by amphiboles with few crystals of plagioclase and pyroxene, flakes of biotite and muscovite. Heavy minerals are rare in the surface samples and recorded in the deeper samples. The deepest samples encloses high percentage of the heavy minerals.

### *Samples at the surface*

Includes high percentage of amphiboles, (mainly hornblende) iron oxide (goethite), few crystals of garnet, zircon and very fine monazite spot in allanite crystals embedded in silicate mineral.

### *Amphibole, $Ca_2(MgFe)_5Si_8O_{22}(OH)$ :*

Amphipole is one of the green silicate present as euhedral crystals of monoclinic system and prismatic form. Its characterized by dark green color with mild transparency and vitreous luster, Fig (3B).

### *Goethite, $FeO(OH)$ :*

Iron bearing hydroxide mineral, It forms through the weathering of other iron-rich minerals, and thus is a common component of soils, concentrated stream sediments present as concretions with brownish black color, it's brittle characterized by submetallic luster and complete opacity and low magnetism Fig (3A).

**Allanite,  $(Ce, Ca, Y)_2(Al, Fe)_3(SiO_4)_3OH$ :**

Allanite was recorded as an accessory mineral in granites, generally the Ce-rich allanite indicates the much-localized remobilization and concentration of REEs during a late hydrothermal alteration (**Yuanming and Micheals, 1991**). The highest LREE contents relative to the HREE indicating magmatic allanite (**Spurgin et al., 2009**). The studied allanite has been supported by the presence of Nd-rich allanite, the highest Nd content Fig. (3c) relatively at high PH condition, calcium Ca and Si are the most easily solublized and Al in mobile, while Fe is very resistant to desolution and completely precipitated as ferruginous mainly goethite (**Taylor and Eggleton,**

**2001**), the recorded goethite represents the secondary phase and is considered as the main criteria for chemical weathering and reflecting the influence of different weathering stages. This result concides with that of (**Price et al., 2005**).

The breakdown of allanite under surficial weathering (epigene) condition can be described as follows: Allanite + Fluids Cerianete + Monazite + clay minerals + goethite (**Meintzer and Mitchell, 1982**).

**Wood and Rickette (2000)** reported that allanite was most commonly replaced by a LREE-Th phosphate phase possibly disrupted monazite Nd ((Nd, Ce, La, Sm,Th)PO<sub>4</sub>). due to intense weathering.

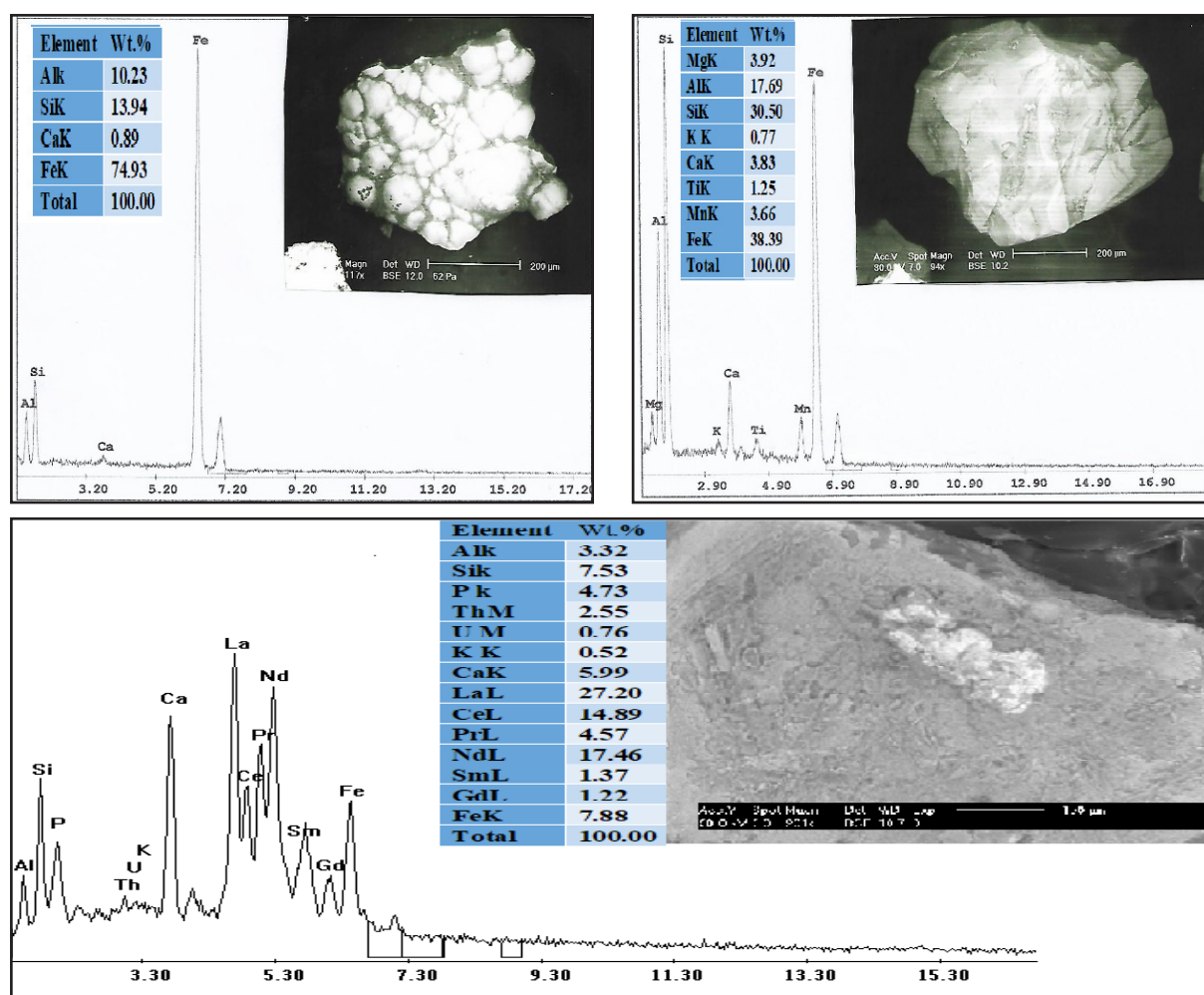


Fig. (3): ESEM image and EDX spectra of a) Geothite, b) Amphibole, c) Allanite at the surface.

**Half meter (0.5m) samples:****Garnet, (Ca, Mg, Fe, Mn)<sub>3</sub>Al<sub>2</sub>Si<sub>3</sub>O<sub>12</sub>:**

In the studied area we find high percentage of garnet Fig. (4a, b), of first and second type pyrope-almandine and almandine-spessartine in addition to zircon of short and long type. The minerals formed during the thermal metamorphism such as garnet, reflecting the mild stress regime during thermal metamorphism. Therefore, the absence of shearing stress in thermal metamorphism allows destroying the almandine garnet and the appearance of spessartite-almandine instead, sometimes before the formation of biotite. Garnet group consist of iron aluminium silicate with chemical formula (Ca, Mg, Fe, Mn)<sub>3</sub>Al<sub>2</sub>Si<sub>3</sub>O<sub>12</sub>, the garnet group can be divided in two sub groups based on different ionic radii of Mg, Fe, Mn on one hand and Ca on the other, the first type pyrope consists of pyrope (Mg, Al)- almandine (Fe, Al) and spessartine (Mn, Al), the second type gronndites include Ca in the structure.

**Xenotime, Y (Po):**

Also, we find xenotime is enriched in HREE (especially Yb, Er, Dy), Y as in Fig. (4c, d). xenotime can be used as a sensitive trace element geothermometer, both with monazite – xenotime pair (**Andres and Heinrich, 1998**). So, after **Ali (2012)**, xenotime from Abu Rusheid lamprophyre dyke formed at a temperature around 600.

**Zircon, (ZrSiO<sub>4</sub>):**

Occurs as euhedral six-sided or eight-sided prismatic crystals. It's mainly colourless to pale yellow. Also, possessing various colours reddish brown-reddish orange. **Vavra (1990)** proposed that zircon shape is a function of conditions of environment of crystallization. In particular, formation of bipyramidal faces is related to slow crystallization as Fig. (4e). Also, some of the studied grains show lengthening where a high fluid content causes the prided of zircon crystallization to lengthen (**Pupin et al.,**

**1978**) some crystals show preferential growth of the pyramidal faces at the expense of prismatic one.

**One meter (1m) samples:**

Some samples record existence of uranothorite, columbite with Nb - Ta ratio (54.48 – 3.89), Also we notice presence of cassterite (SnO<sub>2</sub>) and tourmaline.

Tourmaline, (Ca, K, Na)(Al, Fe, Li, Mg, Mn)<sub>3</sub>(Al, C, Fe, V)<sub>6</sub>(BO<sub>3</sub>)<sub>3</sub>(Si, Al, B)<sub>6</sub>O<sub>18</sub>(OH,F)<sub>4</sub>:

Crystalline boron silicate mineral compounded with elements such as aluminium, iron, magnesium, Na and Li of potassium, of trigonal crystal system with variety of colors most commonly black but can range from colourless to brown red Fig. (4f).

Crystallization immediately after the main phase of crystallization of acidic melts adjacent to the contact rocks, (tourmalization at the expense of biotite) as pneumatically formed mineral in contact metamorphism, tourmaline occur in most granitic, pegmatites and quartz, tourmaline veins and is a common mineral in most medium to high grade metamorphic rocks with topaz-beryl-cassterite fluorite.

**Uranothorite, Th, U (SiO<sub>4</sub>):**

The studied uranothorite generally occurs as the anhedral opaque mineral grains vary in color from dark brown to black and exhibiting submetallic to greasy luster Fig.(5a), the ESEM analysis shows it consists essentially of ThO<sub>2</sub> and SiO<sub>2</sub> which exceeds significantly UO<sub>2</sub>. According to **Heinrich (1958)** uranium is usually present in amounts up to 10% in this mineral. Trace elements of Ca, Al and P, Fe and Y occur in more abundant amounts Fig. (5a).

**Columbite, (Fe, Mn, Mg) (Nb, Ta)<sub>2</sub>O<sub>6</sub>.**

Several columbite crystals have been subjected to semiquantitative analyses and the obtained SEM data show that both Nb and Fe are the essential component together with minor of Ta, Th, U, Na, K and Mg. The grains are black in colour and possess brilliant metallic luster under binocular microscope. The

grains are present in the form of massive rounded to subrounded containing surface cavities, Fig. (5b). The second variety occurs in form of irregular grains

Fig. (5c). Indeed Nb and Ta mineralization are generally associated with Hf-rich zircon.

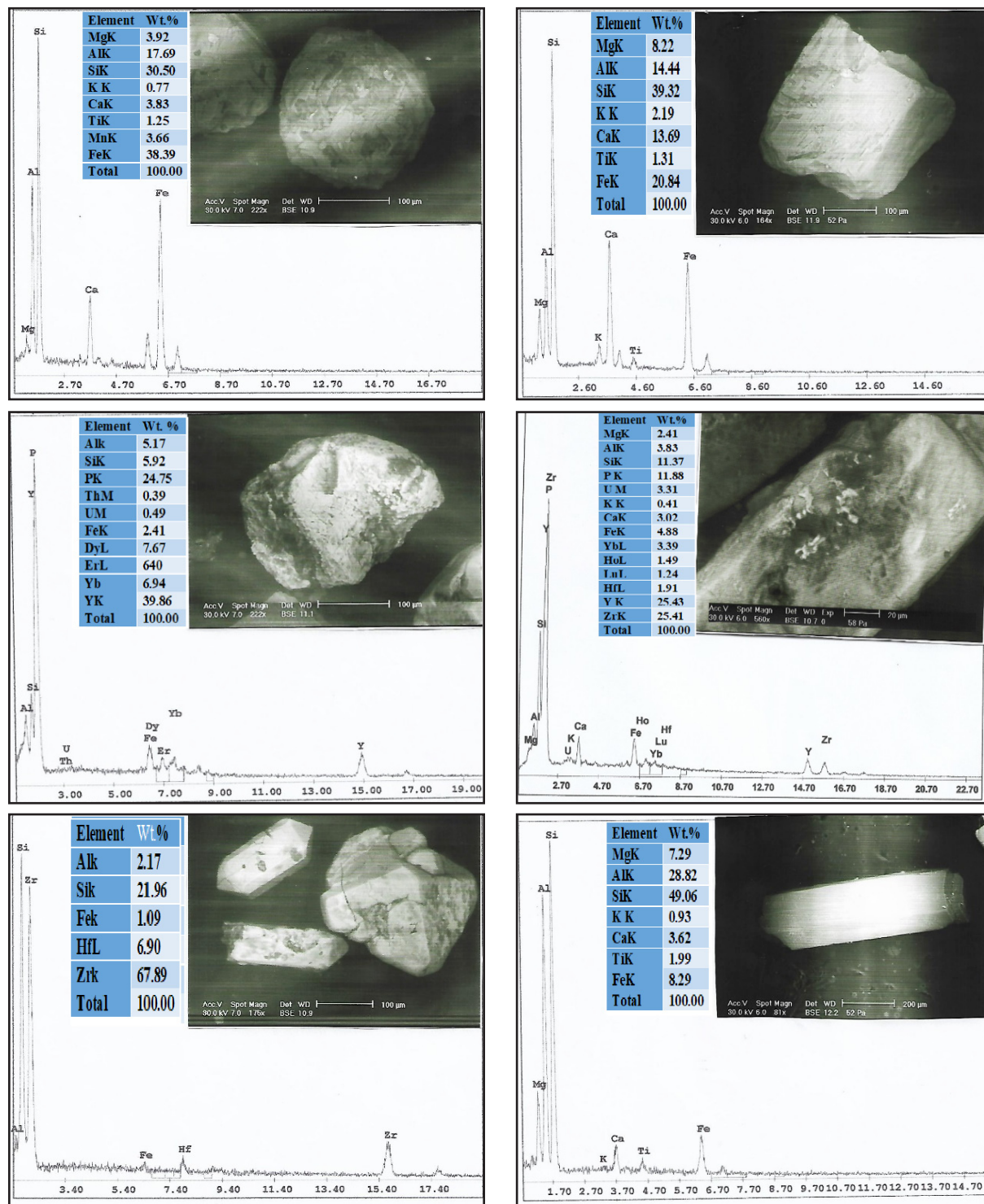


Fig. (4): ESEM image and EDX spectra of a) Garnet Pyrope – Almandine, b) Garnet Almandine spessertine, c) Xenotime, d) Xenotime in Zircon at depth 0.5 m, e) Short + long Zircon at depth 0.5 m, f) Tourmaline at depth 1m.

**Cassterite, (SnO<sub>2</sub>):**

It is a tin oxide mineral, generally opaque but it's translucent in thin crystals, its luster and multi-

ple faces produce a desirable gem, has formula SnO<sub>2</sub> and crystal system tetragonal. Tin shows a chemical similarity to both of it's neighbours in group 14, germanium and lead Fig.(5d).

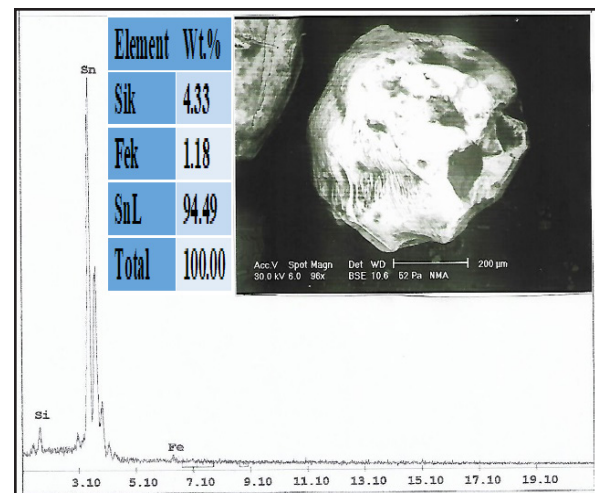
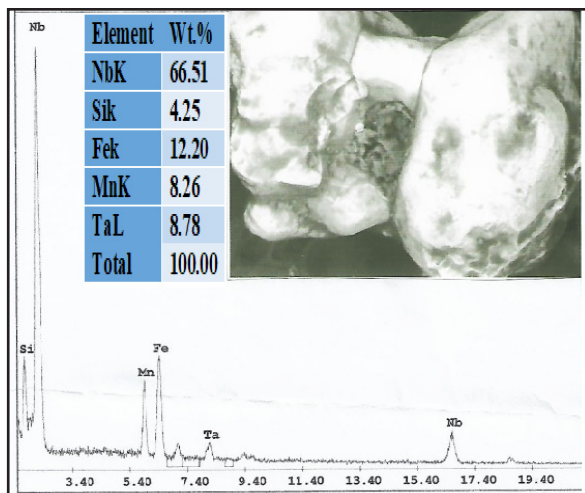
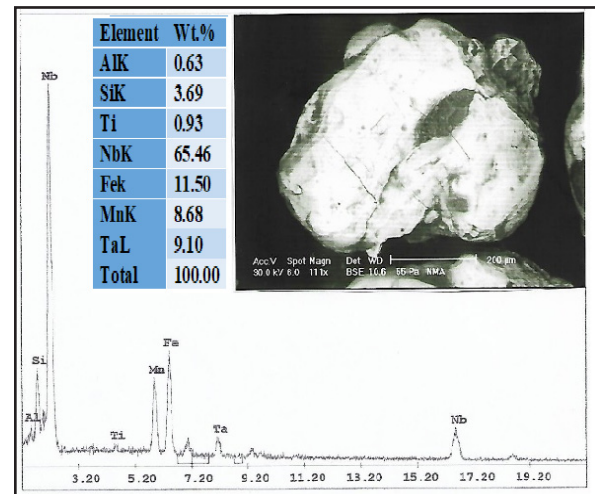
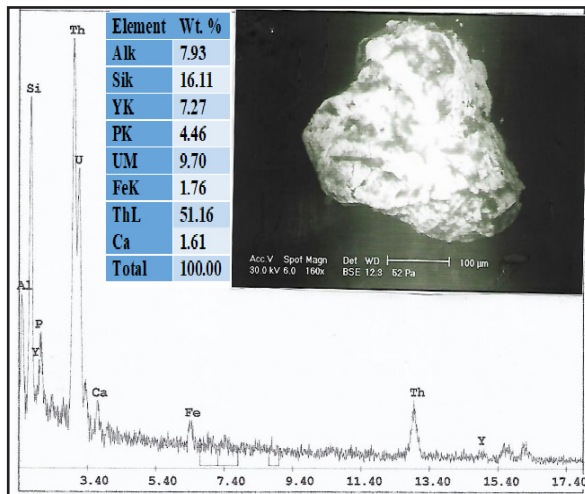


Fig. (5): ESEM image and EDX spectra of a) Uranothorite, b) Columbite, c) of Columbite, d) Cassterite at depth 1m.

**One and a half meter (1.5 m) samples:**

At the end of one meter and half (1.5 m) we can identify zircon bipyramid with ratio of HF (1.97) and Thorite (Th SiO<sub>4</sub>) in addition to garnet and columbite. So that, Zr and Th are generally considered as highly immobile elements.

**Zircon, (ZrSiO<sub>4</sub>):**

While the formation of the prismatic faces is a

function of temperature and degree of zirconium supersaturation in the liquid. However, **Speer (1982)** concluded that it is difficult to relate the morphology to any condition Fig. (6a).

**Thorite, ThO<sub>2</sub>(SiO<sub>2</sub>):**

A common radioactive mineral brown to black in colour, The ESEM analysis shows that thorite consists essentially ThO<sub>2</sub> and SiO<sub>2</sub>. Other elements detected in small to minor amount are Ca, Mg, P, Si

and Fe, whereas rare earth were not detected in the analysed thorite Fig.(6b). According to **Fron del and Cuttito (1955)**, thorite form hydrothermally over

temperature range (300 C to 700 C),the formation of thorite is favoured by acid condtion.

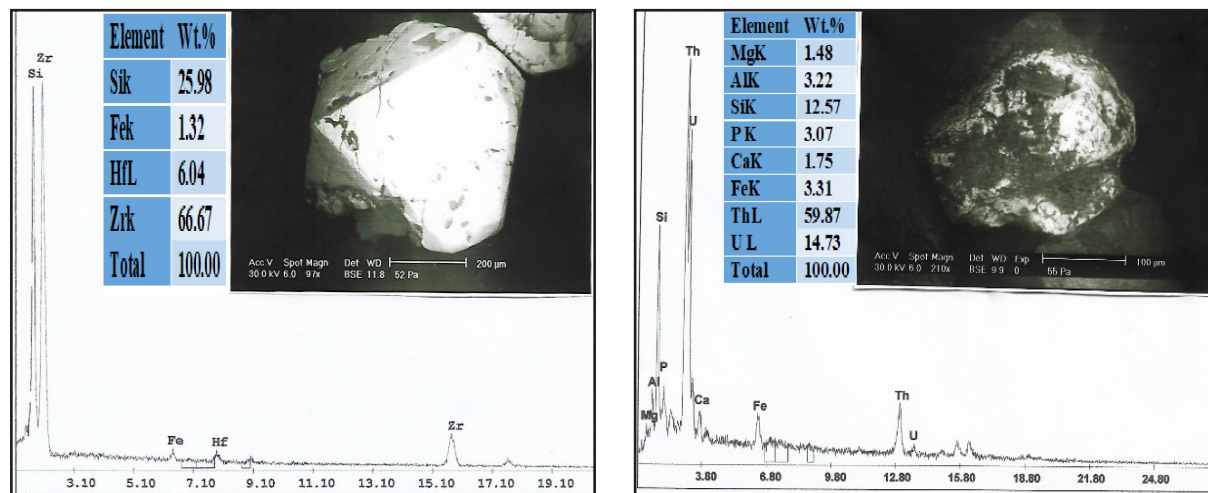


Fig. (6): Show ESEM image and EDX spectra of a) short Zircon, b) Thorite at depth 1.5m.



Fig. (7): Show some minerals under binocular microscope.

**Geochemical studies:**

The elements AL, Ti, Zr, HF, Th, Ga, Cr and REE are considered immobile elements during alteration processes (Maclean and Kranidiotis, 1987; Liaghat *et al.*, 2003 & Calagari and Abedini, 2007). So, in the study area trace elements are richer in Zr, Nb, Y, Sr, Ba, V and Cr, some diagrams are drawn

to indicate the relation between some elements as shown in table (1).

Zr and Y increases with Nb increasing Fig. 8(b, e). While, Y slightly increase with Zr increase Fig. (8d) and Y with vanadium show increase relation Fig. (8c) also. While, Ga increase and vanadium decrease Fig. (8a).

**Table (1) :** Trace elements concentration in ppm of the studied Abu Rusheid stream sediment.

Sample size	Cr	Ni	Cu	Zn	Zr	Rb	Y	Ba	Pb	Sr	Ga	V	Nb
6-1 -0.25	30	25	9	47	134	u.d	37	91	19	6	15	10	22
6-1 -0.5+0.25	447	116	13	146	2642	33	1592	6781	24	141	22	170	497
6-1 -1+0.5	373	140	14	168	1639	47	775	4916	23	86	15	130	306
6-2 -0.25	541	80	10	116	5011	5	2310	>10000	26	266	20	217	947
6-2 -0.5+0.25	359	117	12	149	1831	36	871	5731	23	98	14	154	342
6-2 -1+0.5	481	98	13	148	3122	11	1444	9747	28	165	19	214	587
6-6 -0.25	578	78	9	138	6407	2	3019	9895	42	336	35	238	1208
6-6 -1+0.5	456	134	15	218	4026	48	1909	6147	58	212	43	155	756
6-8 -1+0.5	674	157	6	279	8720	95	4083	4808	138	461	110	124	1639
8-1 -0.5+0.25	380	101	12	133	1200	20	269	7694	21	63	13	204	223
8-3 -0.5+0.25	423	97	10	132	2277	24	1085	6999	31	122	25	188	427
8-4 -0.5+0.25	560	88	12	143	3714	9	1764	>10000	31	198	26	262	698
8-5 -0.5+0.25	480	76	9	131	3451	11	1637	9156	34	181	30	236	647
8-6/1 -0.5+0.25	739	163	u.d	445	>10000	32	>10000	2026	287	1416	254	66	5227
8-6/10 -0.5+0.25	1043	140	u.d	305	>10000	u.d	>10000	5210	343	2123	291	145	7909
8-6/100 -0.5+0.25	822	112	u.d	366	>10000	u.d	>10000	5973	339	2223	303	145	8320
9/1 -0.5+0.25	1093	195	3	642	>10000	137	>10000	1327	380	1513	313	50	5556
9/4 -0.5+0.25	491	147	16	254	5157	63	2442	5439	81	274	63	136	966

9/10 -0.5+0.25	906	165	u.d	1356	>10000	89	8420	1107	340	942	274	47	3419
9/100 -0.5+0.25	903	153	u.d	328	>10000	23	>10000	945	367	1311	301	42	4848
8-1 -0.25	339	113	16	126	1917	22	908	5792	17	98	24	133	350
8-1 -1+0.5	374	114	16	134	1729	19	818	7694	25	86	22	171	314
8-2 -0.25	679	76	14	110	6394	11	3017	1045	33	330	26	240	1179
8-2 -1+0.5	388	117	12	127	3009	37	1426	5526	25	156	21	125	553
8-3 -0.25	582	92	13	138	7007	9	3304	>10000	29	356	33	221	1287
8-3 -1+0.5	322	117	9	124	1973	41	936	5625	27	100	21	140	360
8-4 -0.25	428	75	6	100	5280	8	2493	9718	28	275	19	223	969
8-4 -1+0.5	417	103	11	130	2786	30	1322	7153	28	142	26	179	509
8-5 -0.25	507	77	5	103	5337	9	2521	>10000	33	271	23	245	981
8-5 -1+0.5	356	104	11	143	2219	42	1055	6093	30	111	21	159	404
8-6/1 0.25	781	133	U.D	217	>10000	U.D	9979	5557	187	1061	183	125	3952
8-6/1 -1+0.5	755	167	U.D	345	>10000	73	>10000	2349	384	2543	382	61	>10000
8-6/10 0.25	627	119	U.D	229	>10000	U.D	>10000	5471	194	1090	183	122	4063
8-6/10 -1+0.5	809	142	U.D	300	>10000	97	>10000	3907	305	1965	300	93	7306
8-6/100 0.25	612	129	U.D	220	>10000	20	8374	5044	176	882	155	123	3315
8-6/100 -1+0.5	625	123	U.D	331	>10000	45	>10000	4170	345	2348	340	96	9068
'9/1 -0.25	853	137	U.D	231	>10000	U.D	>10000	4484	189	1062	181	106	3985
'9/1 -1+0.5	990	303	U.D	761	>10000	217	>10000	1118	313	1366	297	42	5032
9/4 -0.25	395	91	4	128	7433	12	3498	8268	50	376	46	194	1367
'9/100 -0.25	781	158	U.D	238	>10000	U.D	>10000	3705	306	1118	275	95	4281
'9/100 -1+0.5	989	189	8	503	>10000	108	>10000	1023	442	1407	424	45	5220

All sample number in size 0.25, -0.5 + 0.25, - 1.0 +0.5, while 8-6/1, 9/1 and <sup>9</sup>/4 → represents sizes on depth 0.5m, 8-6/10 and <sup>9</sup>/10 → represents sizes on

depth 1m, 8-6/100 and <sup>9</sup>/100 → represents sizes on depth 1.5m

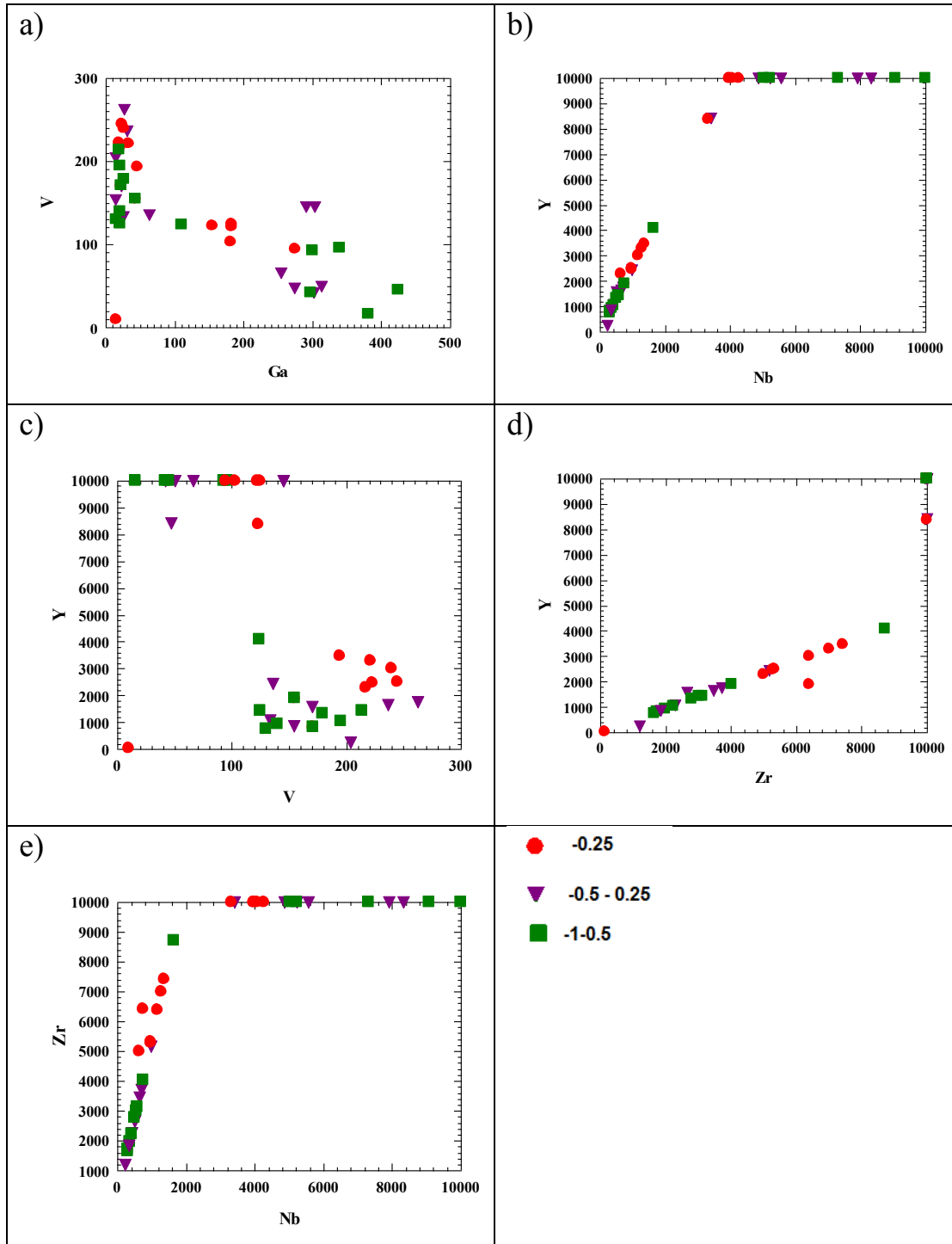


Fig. (8): Binary diagram shows: a) V & Ga, b) Y & Nb, c) Y & V, d) Y & Zr, e) Zr & Nb.

The results of chemical analysis for 17 samples representative the stream sediments in table (2) and relation between uranium and thorium are drawn with some trace elements Fig. (9). Uranium show strong (+ve) relation with Zr, Nb, Y, Ga and slightly (+ve) relation with Pb, and irregular relation with

Zn. While thorium show gently positive relation with Zr, Y, Nb, Pb, Ga and irregular relation with Zn. Uranium show relatively increase in 0.5m and 1m depth respectively while Th increase at 0.5m, 1m and 1.5m with the position of sample.

**Table (2) :** Chemical concentration of uranium, thorium in ppm.

Serial No.	Sample No.	U ppm	Th ppm
1	6-1	300	268
2	6-2	240	225
3	6-6	200	350
4	—	—	—
5	6-8	400	430

#### **REEs distribution:**

The geochemistry of the rare earth elements (REEs) has been intensively studied in the past decades, and that the behavior of the REEs in most geological environments can be accounted for by differences in their ionic radii, (increasing contraction of the 5s and 5p electron shell with increasing atomic mass) as well as variation in valence states ( $Ce^{3+}$  or  $Ce^{4+}$ ,  $Eu^{2+}$  or  $Eu^{4+}$ ). Due to their large ionic radii and charge, the REEs as well as U and Th, behave incompatibly during magmatic process, The LREEs tend to be concentrated in highly fractionated basic rocks such as carbonatites (Forster, 2000).

The REEs in the studied area illustrate more than one depth, samples on the surface have +ve Eu anomaly Fig. (12a), while the middle samples on depth (0.5m, 1m) are similar to each other but differ from surface samples and chondrite Fig. 12(b, c), where they depleted in -ve Eu and Tm. The bottom depth, at (1.5m) europium began to increase, also, Tm which may be an indication to increase in plagioclase Fig (12d). Whilst HREEs increase at (1m) depth where some minerals are concentrated (uranothorite, columbite), otherwise at depth (0.5m)

, (1.5m) HREEs are similar due to the increase in zircon, xenotime, garnet and thorite. (Ibrahim *et al.*, 2007a) recorded the occurrence of REEs up to (1.5%) in the studied lamprophyre dikes in Abu Rusheid. Microscopically lamprophyre dikes ( $L_1$  and  $L_2$ ) are mainly composed of plagioclases, amphiboles, phlogopite, and relics of pyroxenes phenocrysts embedded in a fine-grained groundmass. Xenotime, fluorite, chlorite, and opaque are accessories. The feldspars and micas in both  $L_1$  and  $L_2$  lamprophyres are partially altered to clay minerals (chemical traps) while the oxidation of sulphide minerals left ocelli (physical traps), usually filled by calcite and U minerals (Ibrahim *et al.*, 2015).

Since we find mainly the composition of the studied stream sediment samples table (3), similar petrographically to the altered lamprophyre dikes after (Ali, 2012; Ibrahim *et al.*, 2015). In comparison with the previously mentioned, In addition the NNW-SSE lamprophyre dikes ( $L_1$  and  $L_2$ ) are located in the core of the cataclastic rocks (Ibrahim, 2015). The cataclastic rocks (peralkalic granitic gneisses) are cross cut by NNW-SSE trending altered

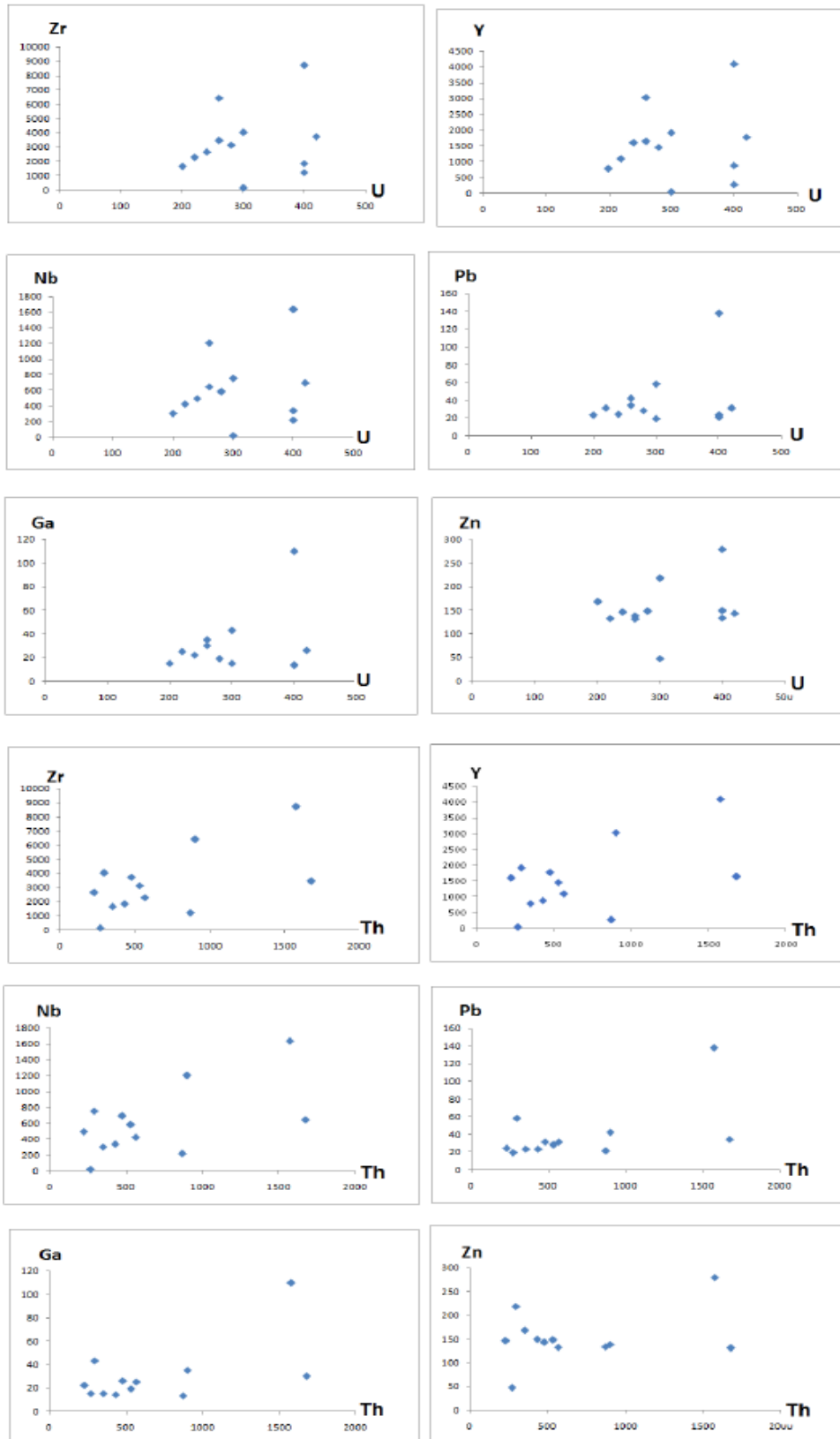


Fig. (9): The relation of U, Th with some trace elements.

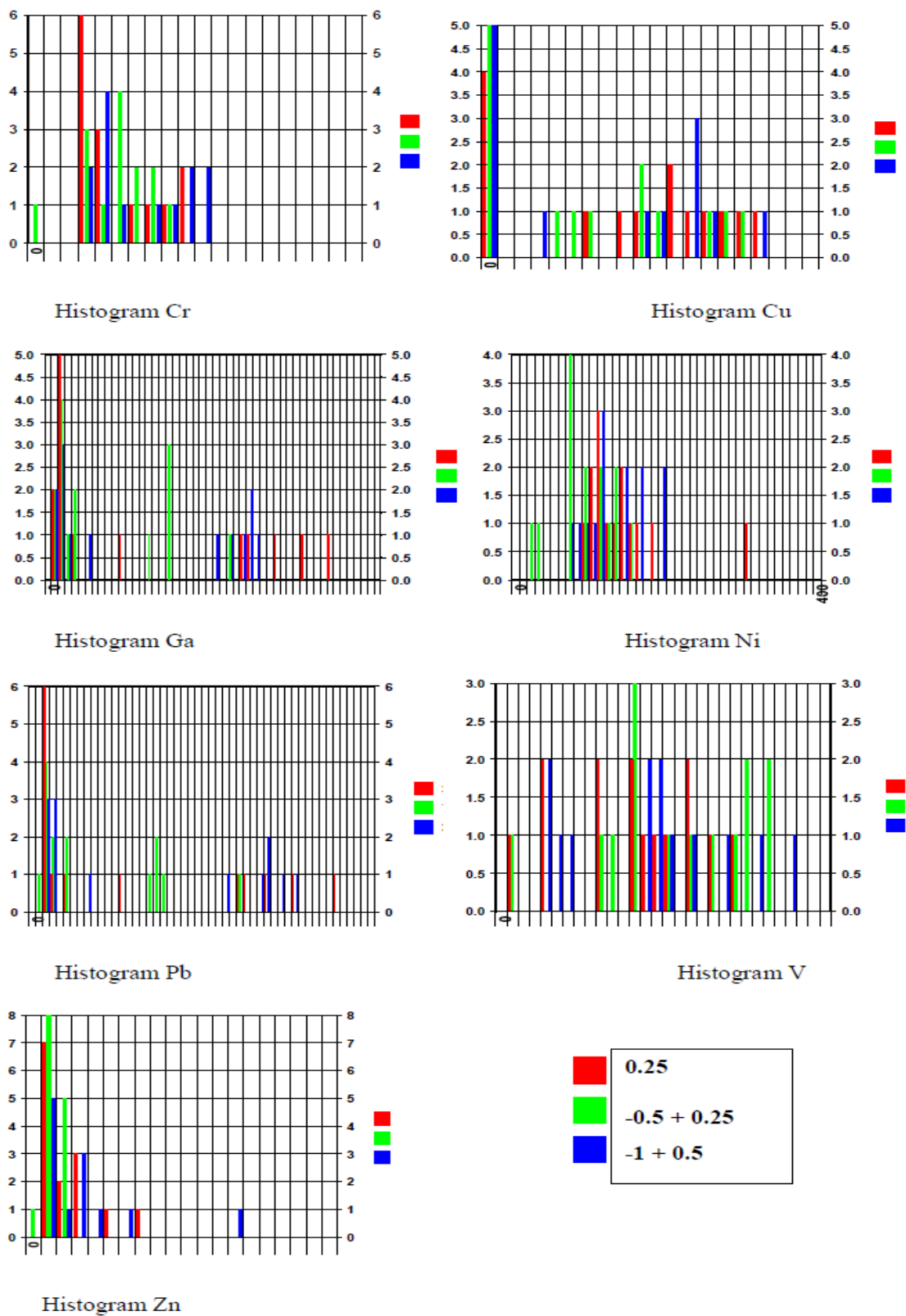


Fig. (10): Histogram show Cr, Cu, Ga, Ni, Pb, V and Zn grain sizes.

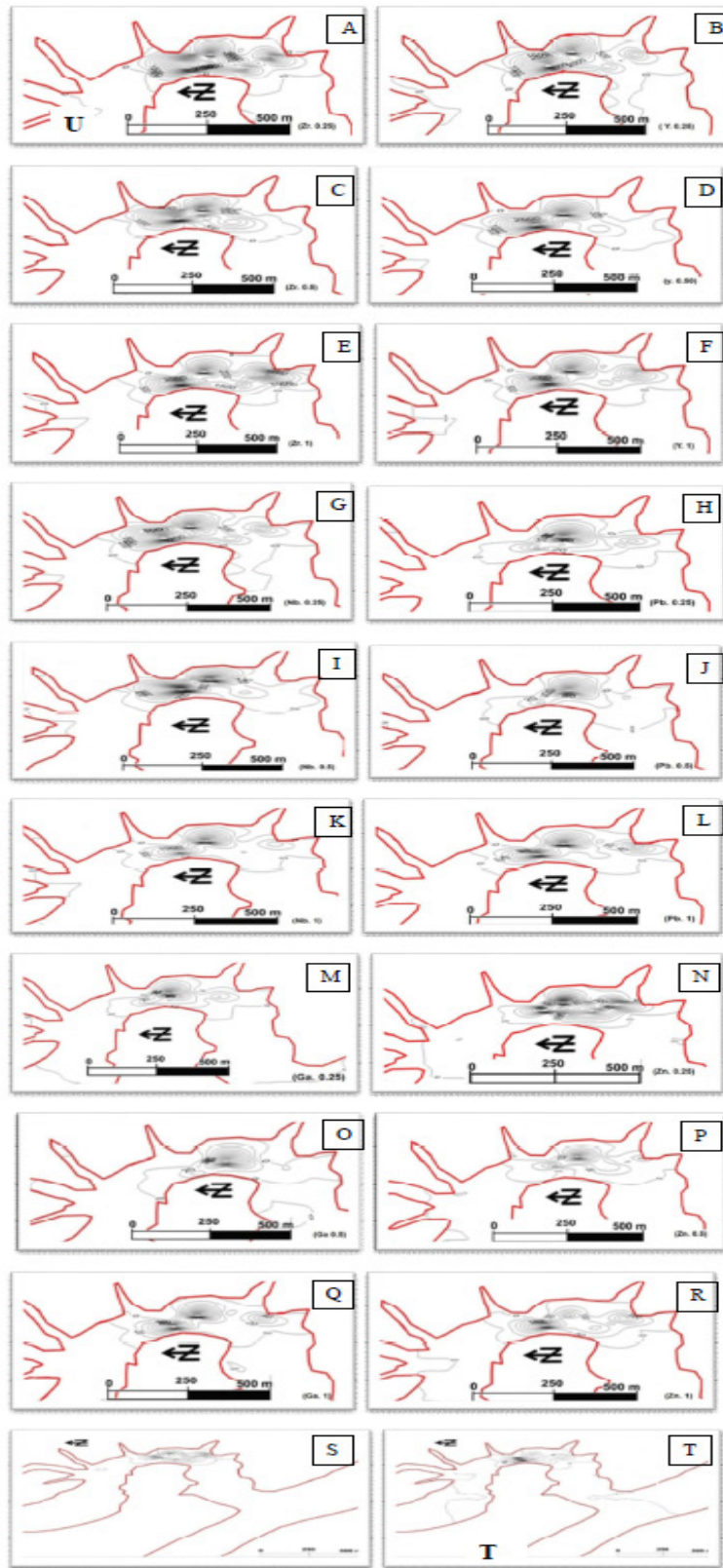


Fig. (11): Contour maps in grain sizes of Zr (A, C, E), Y (B, D, F), Nb (G, I, K), Pb (H, J, L), Ga (M, O, Q), Zn (N, P, R), U (S) and Th (T).

and mineralized shear zone, the lamprophyre dikes were emplaced along shear zone filling in fracture planes (Ali, 2012). The author in the present study suggests that lamprophyre dike for example, ( $L_1$  and

$L_2$ ) with granitic gneisses shear zone is responsible for the increase of REEs percentage in the stream sediment study area.

**Table (3) :** Average of REEs on surface, at 0.5m, at 1m and 1.5m of stream sediment (in ppm) in Abu Rusheid.

Elements n = 3	Average on surface n = 3	at 0.5m n = 3	At 1m n = 3	At 1.5m n = 3	Lamprophyres $L_1+L_2$
La	145.05	146.4	150.13	13.03	199
Ce	9.79	465.49	158.19	565.43	192
Pr	13.2	62.32	30.46	64.52	110
Nd	<0.01	1081.5	2797.72	659.67	340
Sm	<0.01	<0.01	<0.01	3.61	141
Eu	0.74	<0.01	<0.01	0.05	4
Gd	32.59	45.81	64.32	60.07	167
Tb	<0.01	<0.01	<0.01	<0.01	71
Dy	14.36	89.18	114.12	92.09	689
Ho	0.007	<0.01	<0.01	<0.01	174
Er	4.916	5213.44	10360.61	3171.95	843
Tm	0.43	<0.01	<0.01	115.6	137
Yb	4.07	189.77	272.9	185.82	1018
Lu	0.99	34.99	51.08	33.98	151
$\Sigma$ LREEs/ $\Sigma$ HREEs	2.8	0.32	0.29	0.36	0.14

*N* number of samples, <0.01 under detection limits – Lamprophyres comparison after (Ibrahim et al., 2015).

#### **Controlling factors of the REEs distribution:**

In surficial environments, although, it is believed that REEs show low mobility and are resistant to fractionation during weathering processes.

First factor, weathering of minerals parent rocks causes mobilization of elements and fractionation of LREEs and HREEs of Ce and / or Eu (Maclean et al., 1997; Hill et al., 2000 and Patino et al., 2003).

Second factor; PH is the dominant parameter

controlling REEs mobility, under acidic conditions REEs are easily removed from weathering products, absorbed on all types of minerals and amorphous surface coating during koalinization and lateritization, fixed by major scavengers under neutral to alkaline conditions (Nesbitt, 1979 and Fleet, 1984).

(i) The chondrite normalized REEs patterns of all samples, it is reported that Ce is usually retained in the upper parts of the weathering profiles due to the oxidation of Ce (III) to Ce (IV), (Nyakariu et al.,

2001 and Compton *et al.*, 2003). We notice slight negative Ce anomalies and higher in other light elements REEs content. Otherwise, some samples contrastingly, where the REEs pattern has positive Ce anomalies. This may be explained by combined effect of selective remobilization of Ce (IV) could have been initiated during cycles of the stream sediments where chemically reworked.

At the surface and (0.5m and 1m) depth, the negative correlation of Ce could be the result of the two stages, the first stage, Ce might have been positively correlated with Fe scavenging of REE by Fe oxyhydroxides is a wide spread phenomenon (Bau *et al.*, 1996; De Carlo *et al.*, 1998; Bau 1999 & Ohta and Kawabe, 2001).

Second stage, mainly Ce was mobilized at PH above 8, complexes of Ce (IV) are most stable in acidic environment besides free REE ions (Janssen and Verweij, 2003; Roy and SmyKatz Kloss, 2007 & Steinmann and stille, 2006). Whereas less stable REE (III) complexes are adsorbed by scavengers such as Al-Mg hydro silicates and Ti oxides, In the top layer (surface) this explains the +ve anomalie in Gd, Dy and Er. In addition to high partition coeffi-

cient between Gd, Dy and Er in hornblende (10, 13, 12), respectively (Watson and Harrison, 1983). Fig. (12) Ce (IV) complexation have transported to deeper zones where it is adsorbed or precipitated, nearly at 1.5m depth.

(ii) Enrichment in the middle REEs relative to the light and heavy are REE is chiefly controlled by hornblende. The REEs are compatible in hornblende in felsic and intermediate liquids and the highest partition coefficients are between Dy and Er. Such large partition coefficients mean that even a moderate amount of hornblende, according to (Rollinson, 1993).

(iii) Eu anomalies, samples in the Fig. 12 (b,c) show negative Eu anomaly that may be inherited from the felsic precursor rocks a consequence of preferential leaching of Eu associated with the breakdown of feldspar (plagioclase) in direction of upstream sediment, suggesting that plagioclase free sediments are downstream in the studied area (Taylor and McLennan 1988; White *et al.*, 2001 and Villaseca *et al.*, 2003), samples on depth suggests the same source of formation. These relationships are explicable when assuming deposition of stream sediment of Abu Ruheid, (Ozturk *et al.*, 2002).

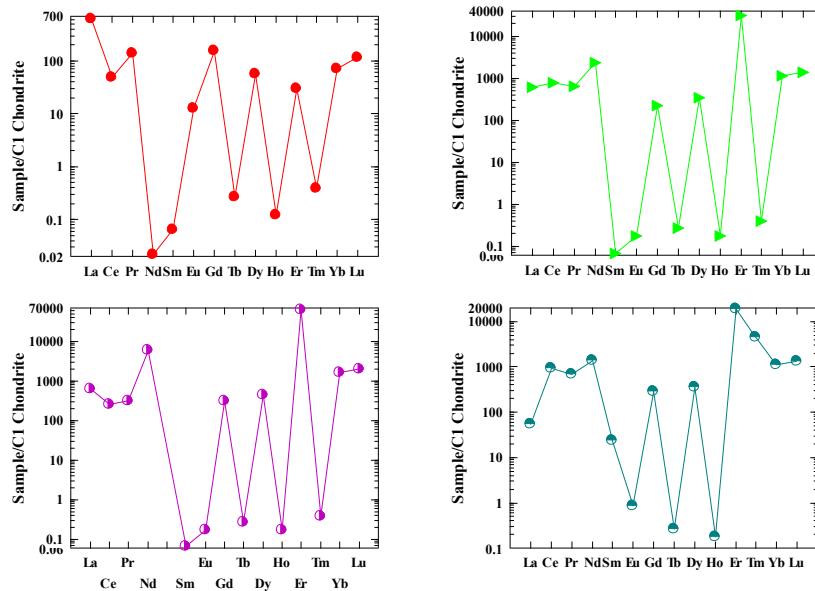


Fig. (12): Chondrite-normalized REEs patterns for the stream sediments, (a) average samples on surface, (b) samples at 0.5m depth, (c) samples at 1m depth, (d) samples at 1.5m depth, Abu Rusheid area, South Eastern Desert, Egypt. Normalizing chondritic values after (Sun, 1980).

## CONCLUSION

(i) The data obtained in this study proved that controlling factors of distribution of rare earth elements and mobility of U, valuable radioelements come from leaching of more labil REEs bearing minerals from granitic gneisses rocks cut by mineralized shear zone and green silicates mainly amphiboles (hornblende). Part of the studied stream sediments samples composition is petrographically similar to the altered lamprophyre dike which is mainly composed of plagioclase, amphibole (H.b), relics pyroxenes, muscovite and chlorite, in addition; the cataclastic rocks (peralkalic granitic gneisses) are cross cut by NNW-SSE trending altered and mineralized shear zone (Ali, 2012). From the comparison of the REEs in the studied stream sediments resembles those of the studied lamprophyre dikes ( $L_1$  and  $L_2$ ) Ibrahim et al., (2015), since we find the majority of minerals in the surface samples of stream sediments for example, amphibole (hornblende), allanite, geothite, few pyroxene, few garnet. Under surficial weathering (epigene), the breakdown of allanite give monazite, clay minerals, cerianite and geothite where Ce and Nd rich allanite indicate concentrated LREEs during a late hydrothermal alteration, while recorded geothite on surface represents the secondary phase and is considered as the main criteria for chemical weathering.

So, under acidic condition REEs are easily removed from weathering product, adsorbed on all types of minerals and amorphous surface coating during kaolinization and lateritization fixed by major scavengers under neutral to alkaline condition.

(ii) Geochemical study of drawing binary relations of U, Th and some trace elements clarified that uranium increase with Zr, Nb, Y, Zn, and slightly increase with Ga and Pb. While thorium show accumulation at the beginning with Zr, Y, Nb, Ga then show dispersed relation with Pb, Zn.

(iii) In addition, histograms show that Ga, Zn and Pb are rich in grain size 0.25 mm and -0.5 + 0.25 while other elements (Cr, Ni, Cu, and V) are moderately rich in all size.

(iv) On the basis of the trace elements content we drawn the geochemical contour maps to explore the mineralization extension in deep levels from surface (0.5m, 1m, 1.5m) of stream sediments according to distribution in Wadi Abu Rusheid. We notice that valuable trace elements take the same direction of peralkalic granitic gneisses and lamprophyre dikes where Zr, Y, Pb and Ga in size (-1 + 0.5) show the highest concentration in NNW-SSE direction and Nb in size (-0.5 + 0.25) take the same direction, while higher concentration of Zn in size (-0.25) take NE-NW, otherwise U take NW-SE and Th take NW to NS direction.

(v) Finally, by drawing chondrite-normalized patterns, The REEs in the studied area illustrate more than one depth, samples on the surface have +ve Eu anomaly, while the middle samples on depth (0.5m, 1m) are similar to each other but differ from surface samples and chondrite, where they depleted in -ve Eu and Tm. The bottom depth at (1.5m) europium began to increase, also, Tm which may be an indication to increase in plagioclase. Whilst HREEs increase at (1m) depth where some minerals are concentrated (uranthorite, columbite), otherwise at (0.5m) and (1.5m) depth HREEs are similar due to the increase in zircon, xenotime, garnet and thorite.

## ACKNOWLEDGMENT

The author: Thanks to Prof. Dr/ Hamdy Abdualah, Dr/ Anton, Especially grateful for Prof. Dr/ Josef. And Dr/ Ehab Korany.

## REFERENCES

- **Abd El-Monem, A.A. and Hurley, P.M. (1979):** U-Pb dating of zircon from psammitic gneisses, wadi Abu Rusheid-wadi Sikait area, Egypt. In Evolution and Mineralization of the Arabian-Nubian Shield

(Vol. 2), pp. 70 .

- **Abdalla, H.M.; Ishihara, S.; Matsueda, H. and Monem, A.A.A. (1996):** On the albite-enriched granitoids at Um Ara area, Southeastern Desert, Egypt. 1. Geochemical, ore potentiality and fluid inclusion studies. *J. Geoch. Exp.*, 57(1): 127.
- **Ali, M.A. (2012):** Mineral chemistry of monazite-(Nd), xenotime-(Y), apatite, fluorite and zircon hosting in lamprophyre dyke in Abu Rusheid area, South Eastern Desert, Egypt. *Geologija*, 55(1): 93.
- **Ali, M.A.; Lentz, D.R. and Hall, D.C. (2011):** Mineralogy and geochemistry of Nb-, Ta-, Sn-, U-, Th-, and Zr-bearing granitic rocks from Abu Rusheid shear zones, South Eastern Desert, Egypt. *Chinese J. Geochem.*, 30(2): 226.
- **Andrehs, G. and Heinrich, W. (1998):** Experimental determination of REE distributions between monazite and xenotime: potential for temperature-calibrated geochronology. *Chem. Geol.*, 149(1): 83.
- **Bau, M. (1999):** Scavenging of dissolved yttrium and rare earths by precipitating iron oxyhydroxide: experimental evidence for Ce oxidation, Y-Ho fractionation, and lanthanide tetrad effect. *Geochim. Cosmochim. Acta*, 63(1): 67.
- **Bau, M.; Koschinsky, A.; Dulski, P. and Hein, J.R. (1996):** Comparison of the partitioning behaviours of yttrium, rare earth elements, and titanium between hydrogenetic marine ferromanganese crusts and seawater. *Geochim. Cosmochim. Acta*, 60(10): 1709.
- **Beus, A.A. (1962):** Albitized and Greisenized Granites (Apogranites). The USSR Academy of Science, 196 P., Moscow, Russia.
- **Bugrov, V.A.; El-Gadael, A.A., and Soliman, M.M. (1973):** Rare metallic albetites as a new type of mineralization in egypt. *Annals Geol. Surv. Egypt*, 111: 185.
- **Calagari, A.A., and Abedini, A. (2007):** Geochemical investigations on Permo-Triassic bauxite horizon at Kanisheeteh, east of Bukan, West-Azarbaidjan, *Iran J. Geoch. Exp.*, 94(1): 1.
- **Carlo, E.H.D.; Wen, X.Y., and Irving, M. (1997):** The Influence of Redox Reactions on the Uptake of Dissolved Ce by Suspended Fe and Mn Oxide Particles. *Aquatic Geochem.*, 3(4): 357.
- **Compton, J.S.; White, R.A. and Smith, M. (2003):** Rare earth element behavior in soils and salt pan sediments of a semi-arid granitic terrain in the Western Cape, South Africa. *Chem. Geol.*, 3–4(201): 239.
- **El-Afandy, A. H.; Abdalla, H. M.; Assran, H.M.; Abou El Fetouh, A.A. and Moghazi, N.M. (2003):** Evaluation of Placer Deposits of Radioactive and Nuclear Elements at Wadi Abu Rusheid Area, Southern Eastern Desert, Egypt. Internal Report of Nuclear Material Authority, 69 p.
- **El-Afandy, A.H.; Abdalla, H.M.; Aly, M.M., and Ammar, F. (2000):** Geochemistry and Radioactive Potentiality of Um Naggat Apogranite, Central Eastern Desert, Egypt. *Resource Geol.*, 50(1): 39.
- **Fleet, A.J. (1984):** Aqueous and sedimentary geochemistry of the rare earth elements. In: Henderson, P. (Ed.), *Developments in Geochemistry* (Vol. 2), Elsevier, pp. 343.
- **Fletcher, W.K.; Church, M. and Wolcott, J. (1992):** Fluvial-transport equivalence of heavy minerals in the sand size range. *Can. J. Earth Sci.*, 29(9): 2017.
- **Forster, H.J. (2000):** Cerite-(Ce) and thorian synchysite-(Ce) from Niederbobritzsch (Erzgebirge, Germany): implications for the differential mobility of Th and the LREE during granite alteration. *Can. Mineral.*, 38: p. 67.
- **Fritz, H.; Dallmeyer, D.R.; Wallbrecher, E.; Loizenbauer, J.; Hoinkes, G.; Neumayr, P. and Khudeir, A.A. (2002):** Neoproterozoic tectonothermal evolution of the Central Eastern Desert, Egypt: a slow velocity tectonic process of core complex exhumation. *J. Afri. Earth. Sci.*, 34(3): 137.
- **Greiling, R.O.; Ramly, M.E.E.; Rashwan, A.A. and Kamal El Din, G.M. (1993):** Towards a comprehensive structural synthesis of the (Proterozoic) Arabian-Nubian Shield in E.Egypt. In *Geoscientific Research in Northeast Africa* (Heinz Schandelmeier,

- Ulf Thorweihe, pp. 15). Balkema, Rotterdam.
- **Heinrich G.W. (1958):** Mineralogy of radioactive raw materials. McGraw Hill Book Co., New York, 654p.
  - **Hill, I. G.; Worden, R. H. and Meighan, I.G. (2000):** Geochemical evolution of a palaeolaterite: the Interbasaltic Formation, Northern Ireland. *Chem. Geol.*, 166(1): 65.
  - **Hilmy, M.E.; Bayoumi, R.M. and Eid, A.S. (1990):** Geochemistry and mineralization of the psammitic gneiss of the Wadi Abu Rushied, Eastern Desert, Egypt. *J. Afri. Earth Sci.*, 11, 197.
  - **Ibrahim, I.; Saleh, G.M.; Amer, T.; Mahmoud, F.; Abu El Hassan, A.; Ali, M.A.; Azab, M.S.; Rashed, M.; Khaleal, F. and Mahmoud, M. (2004):** Uranium and Associated Rare Metals Potentialities of Abu Rusheid Brecciated Shear Zone II, South Eastern Desert, Egypt [M]. Nuclear Materials Authority, Internal Report, Cairo: 182 p.
  - **Ibrahim, M.E.; Saleh, G.M.; El-Tokhi, M.M. and Rashed. M. (2007a):** A Lamprophyre bearing-REEs in Abu Rusheid area, Southeastern Desert, Egypt. The 7<sup>th</sup> Inter. Confer. Geo., Alex. Uni., pp.30.
  - **Ibrahim, M.E.; Watanabe, K.; Saleh, G.M. and Ibrahim, W.S. (2015):** Abu Rusheid lampro-phyre dikes, South Eastern Desert, Egypt: as physical-chemical traps for REEs, Zn, Y, U, Cu, W and Ag. *Arab J. Geosci.*, 8(11): 9261.
  - **Janssen, R.P.T., and Verweij, W. (2003):** Geochemistry of some rare earth elements in groundwater, Vierlingsbeek, The Netherlands. *Water Res.*, 37(6): 1320.
  - **Liaghat, S.; Hosseini, M. and Zarasvandi, A. (2003):** Determination of the origin and mass change geochemistry during bauxitization process at the Hangam deposit, SW Iran. *Geochem. J.*, 37(5): 627.
  - **MacLean, W. H. and Kranidiotis, P. (1987):** Immobile elements as monitors of mass transfer in hydrothermal alteration; Phelps Dodge massive sulfide deposit, Matagami, Quebec. *Econ. Geol.*, 82(4): 951.
  - **MacLean, W.H., Bonavia, F. F. and Sanna, G. (1997):** Argillite debris converted to bauxite during karst weathering: evidence from immobile element geochemistry at the Olmedo Deposit, Sardinia. *Miner. Depos.*, 32(6): 607.
  - **Mathew, K.J.; Bürger, S.; Ogt, S.V.; Mason, P.M.E.M. and Narayanan, U. I. (2009):** Uranium assay determination using Davies and Gray titration proceedings of The Eighth International Conference on Methods and Applications of Radioanalytical Chemistry (Marc Viii) Kailua-Kona, Hawaii, 5.
  - **Meintzer, R.E. and Mitchell, R.S. (1988):** The epigenetic alteration of allanite. *Can. Mineral.*, 26: 945.
  - **Merczenko, Z. (1986):** Separation and Spectrophotometric Determination of Elements." Harwood, New York, 708 p.
  - **Moghazi, A.M.; Hassanen, M.A.; Mohamed, F.H. and Ali, S. (2004):** Late Neoproterozoic strongly peraluminous leucogranites, South Eastern Desert, Egypt – petrogenesis and geodynamic significance. *Miner. Petrol.*, 81(1–2): 19.
  - **Nesbitt, H.W. (1979):** Mobility and fractionation of rare earth elements during weathering of a granodiorite. *Nature*, 279(5710): 206.
  - **Nyakairu, G.W.A. and Koeberl, C. (2001):** Mineralogical and chemical composition and distribution of rare earth elements in clay-rich sediments from central Uganda. *Geochem. J.*, 35(1): 13.
  - **Ohta, A. and Kawabe, I. (2001):** REE (III) adsorption onto Mn dioxide ( $\delta$ -MnO<sub>2</sub>) and Fe oxyhydroxide: Ce (III) oxidation by  $\delta$ -MnO<sub>2</sub>. *Geochim. Cosmochim. Acta*, 65(5): 695.
  - **Öztürk, H.; Hein, J.R. and Hanilci, N. (2002):** Genesis of the Doğankuzu and Mortaş Bauxite Deposits, Taurides, Turkey: Separation of Al, Fe, and Mn and Implications for Passive Margin Metallogeny. *Econ. Geol.*, 97(5):1063.
  - **Patino, L.C.; Velbel, M.A.; Price, J.R., and Wade, J.A. (2003):** Trace element mobility during spheroidal weathering of basalts and andesites in Hawaii and Guatemala. *Chem. Geol.*, 202(3): 343.

- **Price, J.R.; Velbel, M.A. and Patino, L.C. (2005):** Allanite and epidote weathering at the Coweeta Hydrologic Laboratory, western North Carolina, U.S.A. *Am. Mineral.*, 90: 101.
- **Pupin, J.P.; Bonin, B.; Tessier, M. and Turco, G. (1978):** Role de l'eau sur les caracteres morphologiques et la cristallisation du zircon dans les granitoides. *Bull. Soc. Géol. Fr.*, S7-XX(5): 721.
- **Rollinson, H.R. (1993):** Using geochemical data: evolution, presentation, interpretation. John Wiley and Sons, New York.
- **Roy, P.D. and Smykatz-Kloss, W. (2007):** REE geochemistry of the recent playa sediments from the Thar Desert, India: An implication to playa sediment provenance. *Chem. Erde-Geochem.*, 67(1): 55.
- **Rubey, W.W. (1933):** The size distribution of heavy minerals within a water-laid sandstone. *J. Sediment. Res.*, 3(1): 3.
- **Speer, J.A. (1982a):** Zircon. In: Reviews in Mineralogy (vol. 5: 2<sup>nd</sup> edition) Orthosilicates, Ribbe, P.H. (ed.), pp. 67.
- **Speer, J.A. (1982b):** The actinides orthosilicates. In: Reviews in Mineralogy (vol. 5: 2<sup>nd</sup> edition) Orthosilicates, Ribbe, P.H. (ed.), pp. 113.
- **Spurgin, S.; Selbekk, R. and Lundmark, M. (2009):** Mineralogy and geological setting of allanite (Ce)- pegmatites in western Hurrungane, Jotun Nappe Complex, Norway: an EMP and ID-TIMS study. *Norw. J. Geol.*, 89: 341.
- **Steinmann, M. and Stille, P. (2006):** Rare earth element transport and fractionation in small streams of a mixed basaltic–granitic catchment basin (Massif Central, France). *J. Geoch. Exp.*, 88(1): 336.
- **Sun, S.S. (1982):** Chemical composition and origin of the Earth's primitive mantle, *Geochim. Cosmochim. Acta*, 46: 179.
- **Taylor, G. and Eggleton, R.A. (2001):** Regolith Geology and Geomorphology: John Wiley & Sons, Ltd., New York, 375 p.
- **Taylor, S.R. and McLennan, S.M. (1988):** The significance of the rare earths in geochemistry and cosmochemistry. In: Handbook on the Physics and Chemistry of Rare Earths, (Vol. 11) Karl, A.; Gschneidner, Jr. and L. Eyring (eds.), Elsevier, pp. 485.
- **Vavra, G. (1990):** On the kinematics of zircon growth and its petrogenetic significance: a cathodoluminescence study. *Contrib. Mineral. Petrol.*, 106(1): 90.
- **Villaseca, C.; Martín Romera, C.; De la Rosa, J. and Barbero, L. (2003):** Residence and redistribution of REE, Y, Zr, Th and U during granulite-facies metamorphism: behaviour of accessory and major phases in peraluminous granulites of central Spain. *Chem. Geol.*, 200(3–4): 293.
- **Watson, E.B. and Harrison, T.M. (1983):** Zircon saturation revisited: temperature and composition effects in a variety of crustal magma types. *Earth Planet. Sci. Lett.*, 64: 295.
- **White, A. F.; Bullen, T.D.; Schulz, M.S.; Blum, A.E.; Huntington, T.G. and Peters, N.E. (2001):** Differential rates of feldspar weathering in granitic regoliths. *Geochim. Cosmochim. Acta*, 65(6): 847.
- **Wood, S.A. and Ricketts, A. (2000):** Allanite-(Ce) from the Eocene Casto Granite, Idaho: Response to hydrothermal alteration. *Can. Mineral.*, 38: 81.
- **Yuanming, P. and Michael, E. F. (1991):** Anadian allanite-(La) and anadian allanite-(Ce) from the Hemlo Gold Deposit, Ontario. *Can. Mineral.*, 55(381): 497.